

Kinetic and thermal stability study of hydrogenated cardanol and alkylated hydrogenated cardanol

Germana M. S. Paiva · Alessandra R. Freitas ·
Francisco X. Nobre · Cleide M. S. Leite ·
José M. E. Matos · Maria A. S. Rios

Received: 15 September 2014 / Accepted: 1 February 2015
© Akadémiai Kiadó, Budapest, Hungary 2015

Abstract In the present work, the thermal stabilities and decomposition kinetics of the hydrogenated cardanol and its derivative—alkylated hydrogenated cardanol—were investigated using thermogravimetry. The chemical compounds showed results comparable to butylated hydroxytoluene, a commercial product that has antioxidant activity. The kinetic parameters of activation energy (E), Arrhenius pre-exponential factor (A), thermal endurance, and relative thermal index were described. Different heating rates were used, and the standard test methods—ASTM E1131-08, E1641-13, and E1877-13—were followed. According to the results, the alkylated hydrogenated cardanol showed the highest activation energy $83.02 \times 10^3 \text{ J mol}^{-1}$ and the higher thermal stability, followed by hydrogenated cardanol $40.08 \times 10^3 \text{ J mol}^{-1}$ and butylated hydroxytoluene $33.48 \times 10^3 \text{ J mol}^{-1}$.

Keywords TG · Activation energy · BHT · Cardanol

Introduction

Additives are chemical compounds that aim to enhance specific qualities as well as soften the defects present in many substances, among lubricants [1]. Among various types of additives, dispersants, detergents, anti-corrosives, anti-caking agents, and antioxidants also have a larger number of studies and papers published [2–4].

The phenolic antioxidants and their mono-, di-, and polynuclear derivatives are the main types of antioxidant additives as they are radical sequester, metal deactivators, and hydroperoxide decomposers and still have effect against the degradation of organic material [5–7]. In this respect, Fig. 1 shows the structures of the hydrogenated cardanol (HC), the alkylated hydrogenated cardanol (AHC), and commercial antioxidant butylated hydroxytoluene (BHT), emphasizing the structural similarity of these molecules.

According to Mazzetto [8], the comparative studies on the antioxidant effect of the HC derivatives and commercial products of petroleum derivatives such as BHT have been reported in the literature. The results demonstrate the efficiency of the antioxidant derived from HC [1, 8].

Various thermal studies are used extensively to understand the behavior of the HC derivatives. Thermogravimetry (TG) is a technique that has very prominence. Ionashiro [9] pointed that there are factors that can affect the TG curves, and these factors may be instrumental and even characteristic of the sample itself. In relation to experimental factors, Leiva [10] applied that the flow rates of 50 and 100 mL min⁻¹ have a similar behavior, so the flow of the carrier gas does not influence the degradation process. There are standards that suggest the use of 20–50 mL min⁻¹ for gas flow [11].

G. M. S. Paiva (✉) · A. R. Freitas · C. M. S. Leite ·
J. M. E. Matos
Departamento de Química, Grupo de Inovações Tecnológicas e
Especialidades Químicas, Universidade Federal do Piauí,
Campus Ministro Petrônio Portella, Teresina,
PI CEP 64.049-550, Brazil
e-mail: germana.grintequi@gmail.com

F. X. Nobre · J. M. E. Matos
Departamento de Química, Laboratório Interdisciplinar de
Materiais Avançados, Universidade Federal do Piauí, Campus
Ministro Petrônio Portella, Teresina, PI CEP 64.049-550, Brazil

M. A. S. Rios
Departamento de Engenharia Mecânica, Grupo de Inovações
Tecnológicas e Especialidades Químicas, Universidade Federal
do Ceará, Campus do Pici, Fortaleza, CE CEP 60.440-554,
Brazil

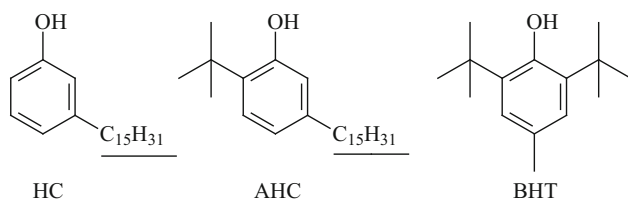


Fig. 1 Chemical structures of HC, AHC, and BHT

Through the data obtained from thermogravimetric curves with different heating rates, various methods have been created to determine the activation energy, which are used by several authors in their studies [11–15]. The methodologies described in ASTM E1641-13 [11] and ASTM E1877-13 [16] use experimental data of thermogravimetric curves for the calculation of the activation energy and thermal resistance, respectively.

In this context, this paper aims to show the thermal efficiency, using data from thermogravimetric curves, activation energy, and the results of thermal resistance for the derivative of HC. The samples of this study were AHC, HC, and BHT. Standard test methods were employed with modifications [11, 16, 17].

Experimental

Materials

The BHT was purchased from Sigma-Aldrich Co ($\geq 99\%$). Hydrogenated cardanol and alkylated hydrogenated cardanol were obtained from Group of Technological Innovations and Chemical Specialties. The HC was obtained by catalytic hydrogenation method [18, 19] and was purified by column chromatography (silica gel) employing hexane as eluant [1]. After being purified, the HC was alkylated by Friedel–Crafts mechanism using *tert*-butyl chloride in the presence of zinc chloride (Lewis acid), obtaining AHC [19]. The HC and AHC were characterized by GCMS (see Figs. 2a, b, 3a, b). The analyses showed the molecular ions at m/z 304 [$C_{21}H_{36}O^+$] and at m/z 360 [$C_{25}H_{44}O^+$], compatible with the molecular formulas of HC and AHC, respectively.

Instrumental

The TG curves were obtained using a thermobalance TA Instrument, model Q 600, in nitrogen atmosphere, with a flow of 50 mL min^{-1} , sample mass of 5 mg, heating rates of 2.5, 5.0, 7.5, and $10.0\text{ }^\circ\text{C min}^{-1}$, and temperature range of 30–800 $^\circ\text{C}$.

Gas chromatography and mass spectrometry were performed by the use of GCMS-QP5050-A (Shimadzu)

equipped with a OV-5 column (0.25 mm, 30 m, $0.25\text{ }\mu\text{m}$ film), electron impact at 70 eV, and the injection and detector temperatures were 250 and 280 $^\circ\text{C}$, respectively; temperature program of the oven starting at 100 $^\circ\text{C}$, increasing to 180 $^\circ\text{C}$ at a rate of $40\text{ }^\circ\text{C min}^{-1}$ and then to 300 $^\circ\text{C}$ at a rate of $10\text{ }^\circ\text{C min}^{-1}$; and helium gas flow as a carrier and volume of sample injected of 1.0 μL .

Methods

Determination of the kinetic parameters

According to ASTM E1641-13 [11], the determination of the kinetic parameters, activation energy, and Arrhenius pre-exponential factor are obtained by TG, based on the assumption that the decomposition obeys first-order kinetics. So, in the present work, the calculation of activation energy was obtained from the plotted graph of $\log \beta$ against $1/T$. The calculation methodology used works with iterations, using Eq. 1 and a value of $0.457/\text{K}$ for b on the first iteration:

$$E = -\left(\frac{R}{b}\right) \times \frac{\Delta(\log \beta)}{\Delta(1/T)} \quad (1)$$

where E = refined Arrhenius activation energy, J mol^{-1} , R = gas constant, $8.314\text{ J mol}^{-1}\text{ K}^{-1}$, β = heating rate, K min^{-1} , T = temperature/K at constant conversion, $\Delta(\log \beta)/\Delta(1/T)$ = slope of the line, and b = approximation derivative from Table 1 (used b $0.457/\text{K}$ on first iteration). The refined activation energy is a parameter obtained by mathematical iterations until the consecutive activation energy values do not show significant differences. So, this refined value is reported as the Arrhenius activation energy.

After obtaining the refined Arrhenius activation energy (E), the value will be used in the relation E/RT_c , where T_c = the temperature at constant conversion for the heating rate closest to the midpoint of the used heating rates. Using the value obtained for E/RT_c , a new estimation of the approximation derivative (b) from Table 1 was obtained, and this new value must be resubmitted to Eq. 1. Iterations should be repeated until the Arrhenius activation energy (E) does not show significant variations [11].

The value of pre-exponential factor will be calculated selecting the mass loss curve for the heating rate nearest the midpoint of the used heating rates, and using Eq. 2 [11]:

$$A = -\left(\frac{\beta'}{E}\right) \times R \times \ln(1 - \alpha) \times 10^a \quad (2)$$

where A = pre-exponential factor, min^{-1} , β' = heating rate nearest the midpoint of the experimental heating rates, K min^{-1} , α = conversion value of decomposition, and a = approximation integral taken from Table 1 [11].

Fig. 2 **a** Chromatogram of hydrogenated cardanol. **b** Mass spectrum of hydrogenated cardanol

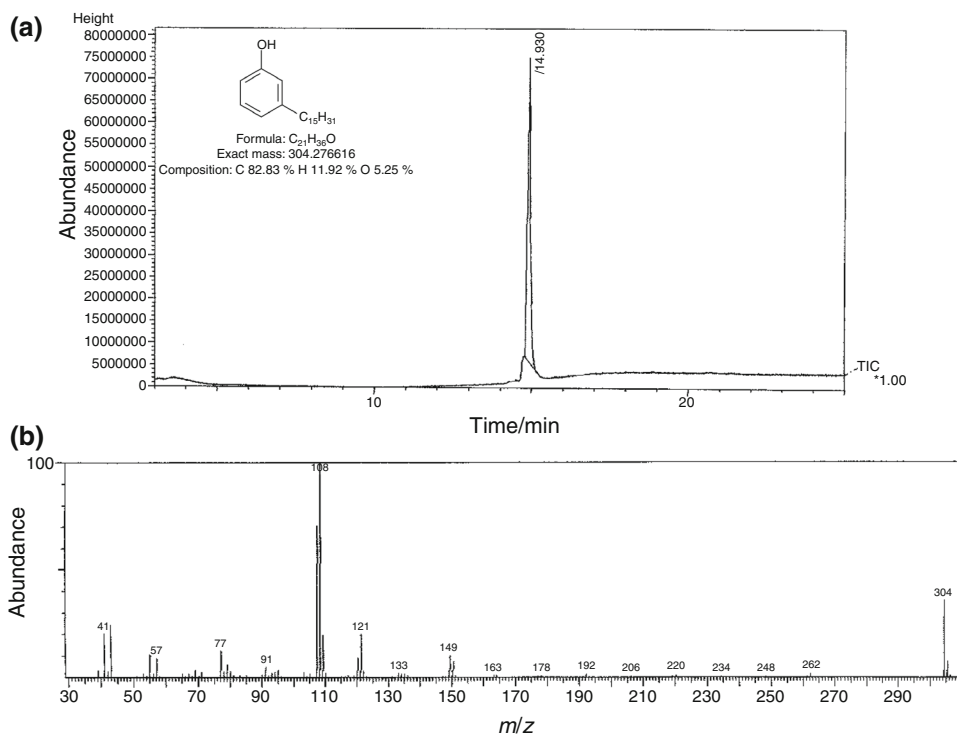
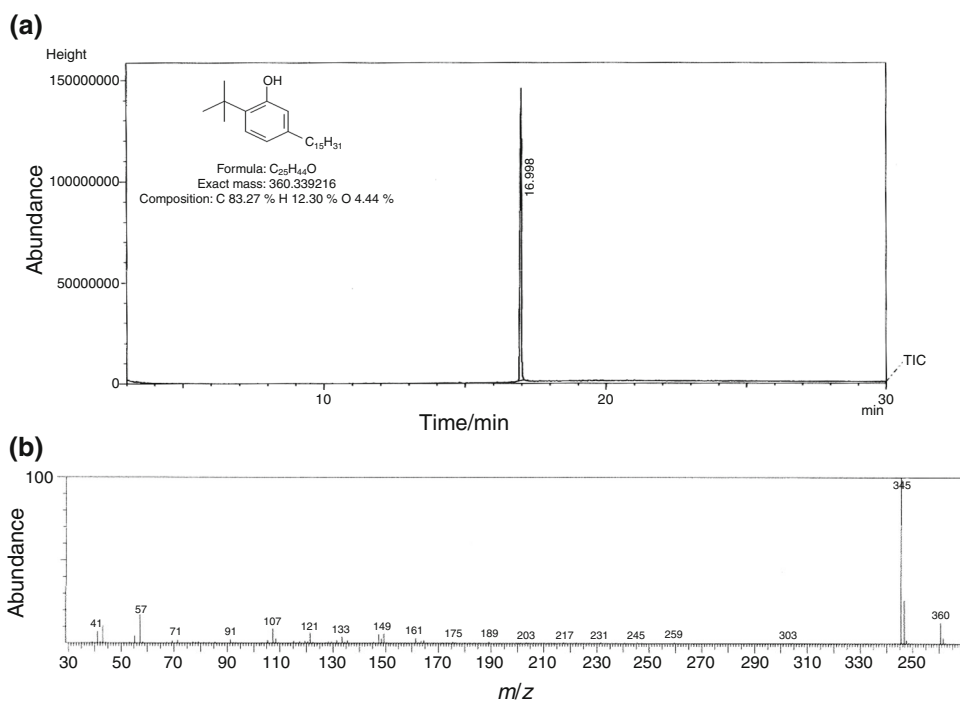


Fig. 3 **a** Chromatogram of alkylated hydrogenated cardanol. **b** Mass spectrum of alkylated hydrogenated cardanol



Calculation of thermal endurance

According to ASTM E1877–11 [11], the methodology presents the additional treatment of the Arrhenius activation energy data to develop a thermal endurance curve and derive a relative thermal index (RTI) for materials [16].

Relative thermal index is a measure of the thermal endurance of a material when compared with that of a control with proven thermal endurance characteristics. In this paper, the thermal endurance, estimated thermal life (t_f), and failure temperature (T_f) were calculated using Eqs. 3 and 4 [16, 20, 21].

Table 1 The numerical integration constants utilized in this work

E/RT	a	b (1/K)
10	6.4167	0.5187
10.79	6.8206*	0.5122*
10.86	6.8564*	0.5121*
11	6.928	0.511
12	7.433	0.505
20	11.3277	0.4770
20.4853	11.5584*	0.4760*
21	11.803	0.475
21.31	12.1296*	0.4744*
22	12.276	0.473

* Obtained by interpolation

ASTM E1641—07 (2013) [11]

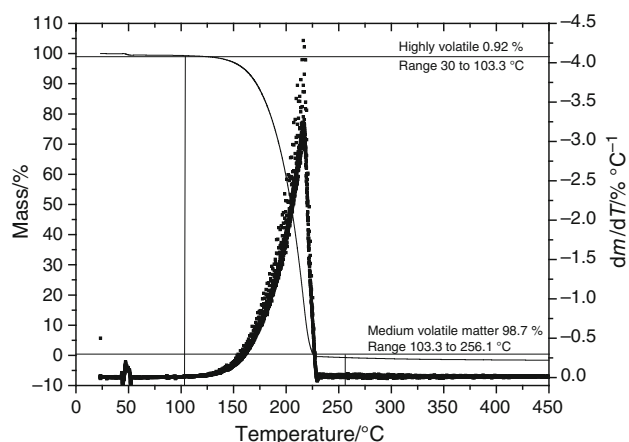
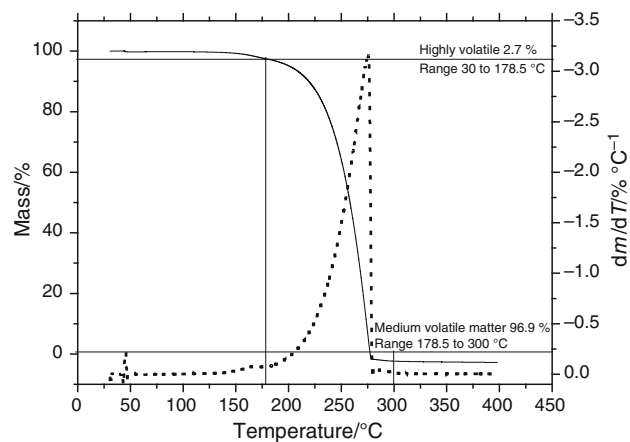
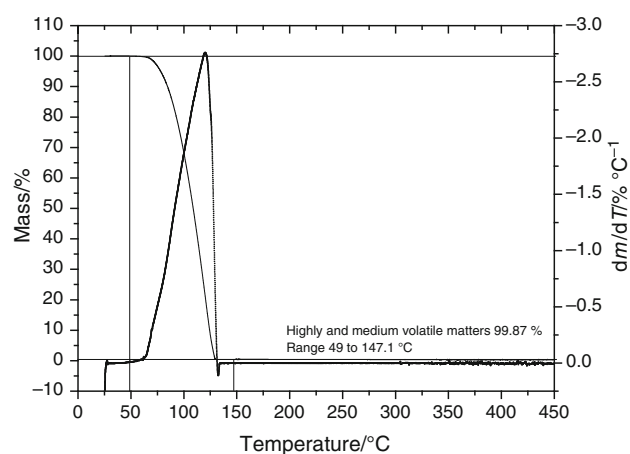
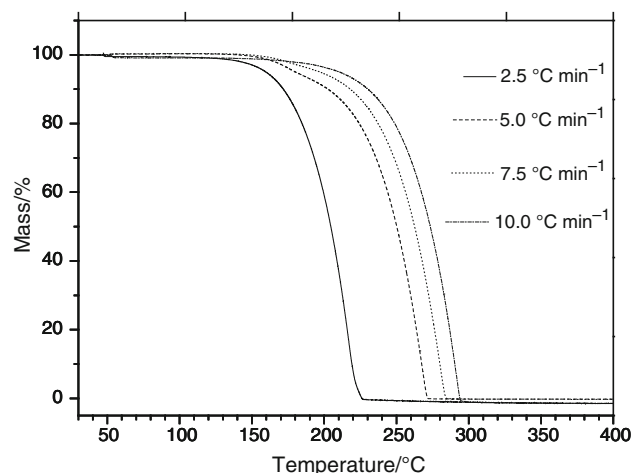
$$\log t_f = \frac{E}{(2.303RT_f) + \left[\log \frac{E}{(R\beta)} \right] - a} \quad (3)$$

$$T_f = \frac{E}{\left(2.303R \left[\log t_f - \log \left\{ \frac{E}{(R\beta)} \right\} + a \right] \right)} \quad (4)$$

where t_f = estimated thermal life for a given value of conversion (α) (min) and T_f = failure temperature for a give value of conversion (α) (K).

Results and discussion

The TG curves of HC, alkyl hydrogenated cardanol (AHC), and BHT are shown in Figs. 4–6. The curves determine the amount of highly volatile matter, medium volatile matter, and the residual weight remaining after the heating [17]. In this procedure, a constant heating rate of $2.5 \text{ }^\circ\text{C min}^{-1}$ was used. According to the results, the HC shows 0.38 % of

**Fig. 4** Thermogravimetric curve of hydrogenated cardanol, $2.5 \text{ }^\circ\text{C min}^{-1}$ **Fig. 5** Thermogravimetric curve of alkylated hydrogenated cardanol, $2.5 \text{ }^\circ\text{C min}^{-1}$ **Fig. 6** Thermogravimetric curve of butylated hydroxytoluene, $2.5 \text{ }^\circ\text{C min}^{-1}$ **Fig. 7** Thermogravimetric curves of the HC (2.5 , 5.0 , 7.5 , and $10.0 \text{ }^\circ\text{C min}^{-1}$)

residual weight remaining after the heating, and the AHC and the BHT show 0.4 and 0.13 %, respectively.

Figures 7, 8, and 9 present the thermogravimetric curves for HC, AHC, and BHT in different heating rates: 2.5, 5.0, 7.5, and 10.0 °C min⁻¹. The thermogravimetric curves

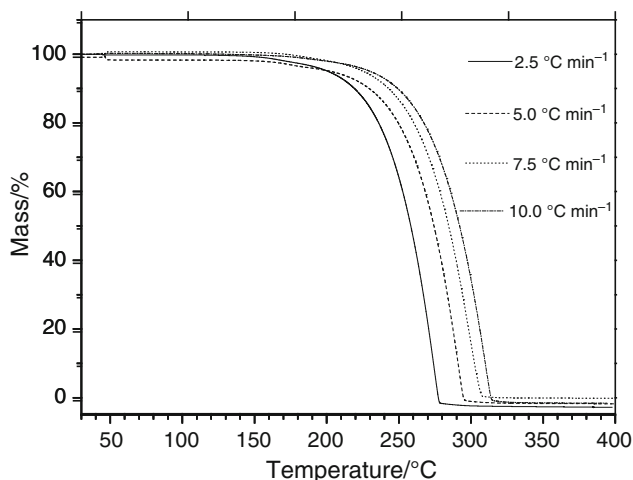


Fig. 8 Thermogravimetric curves of the AHC (2.5, 5.0, 7.5, and 10.0 °C min⁻¹)

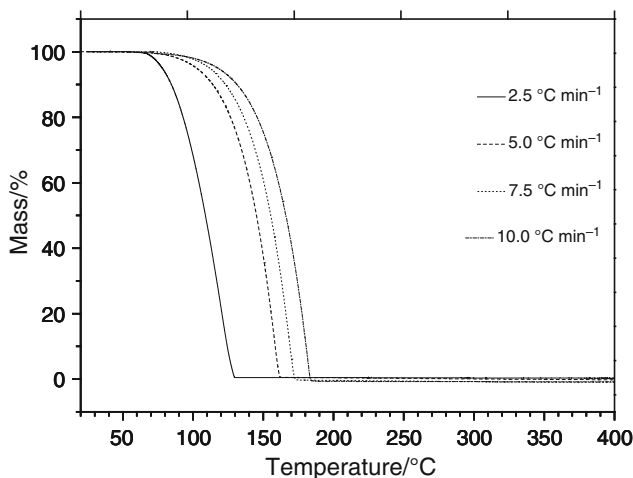


Fig. 9 Thermogravimetric curves of the BHT (2.5, 5.0, 7.5, and 10.0 °C min⁻¹)

indicate with increased thermal stability of AHC, this has the first mass loss temperature >178.5 °C.

In our study, from each thermal curve obtained, an absolute temperature at constant conversion ($\alpha = 0.05$) was determined, see Table 2. After that, the plot of the logarithm of the heating rate expressed as kelvins per minute against the reciprocal of the absolute temperature was obtained (Figs. 10–12) [22, 23].

According to the results, straight lines were obtained, and using the least square method fit, the slopes [$\Delta(\log \beta)/\Delta(1/T)$] of the HC, AHC, and BHT were determined. The calculations of the kinetic parameters—activation energy (E)—were obtained by mathematical iterations, using Eq. 1 for the first calculus. The value of 0.457/K for b was used in the first iteration, see Table 3.

The iterations were executed until the values for the activation energy showed small changes. So, the refined value of 40.08×10^3 J mol⁻¹ was used in the calculation of the pre-exponential factor (A). For the calculus of the pre-exponential factor (A), the mass loss curve for the heating rate nearest the midpoint of the experimental heating rates (5.0 °C min⁻¹) was selected. Eq. 2 was used, and the value of the exponent, a , obtained from Table 1 for the refined value of E/RT_c ($a = 6.8206$). Table 4 presents the parameters for the calculus of (A).

Table 5 shows the kinetic parameters of the AHC and BHT, which followed the same procedure for the calculus of the HC.

The decomposition profiles of the samples were defined by thermogravimetric curves and kinetic parameters such as activation energy (E) and pre-exponential factor (A). According to the TG curves, the temperature range of medium volatile matter of HC varied between 103.3 and 256.1 °C, with refined activation energy of 40.08×10^3 J mol⁻¹, while the AHC and BHT showed temperature ranges of 178.5–300 °C and 49–147.1 °C, and activation energies of 83.02×10^3 and 33.48×10^3 J mol⁻¹, respectively.

According to the TG curves and the calculus of the parameters, the AHC presented the major thermal stability when compared with HC and BHT. This behavior probably occurs because the AHC possesses a phenolic structure, with an *ortho*-substituent in its phenolic ring [24, 25].

Table 2 Temperatures obtained from thermogravimetric curves

Heating rate (β)/K min ⁻¹	Log (β)	HC			AHC			BHT		
		$T/^\circ\text{C}$	T/K	$1/T/\text{K}$	$T/^\circ\text{C}$	T/K	$1/T/\text{K}$	$T/^\circ\text{C}$	T/K	$1/T/\text{K}$
2.5	0.40	160	433	1/433	201	474	1/474	78	351	1/351
5.0	0.70	180	453	1/453	217	490	1/490	103	376	1/376
7.5	0.88	197	470	1/470	226	499	1/499	112	385	1/385
10.0	1.00	211	484	1/484	230	504	1/504	118	391	1/391

Fig. 10 Arrhenius plot of heating rate, temperature of constant conversion data ($\alpha = 0.05$), hydrogenated cardanol

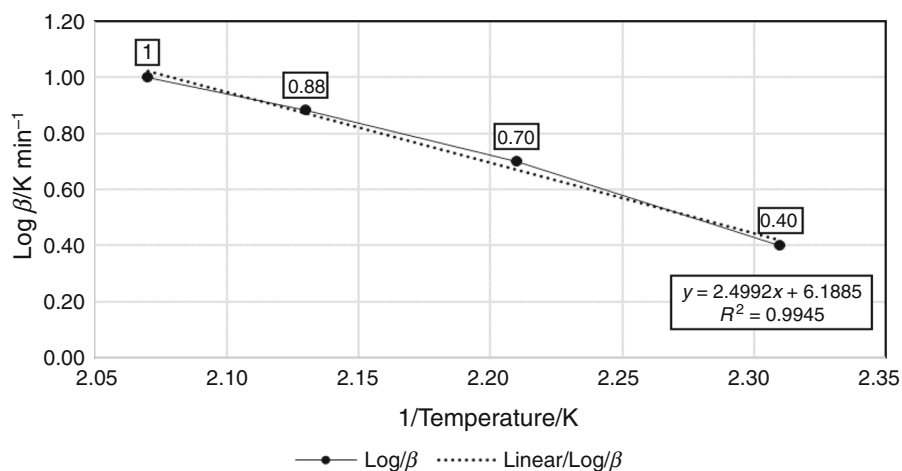


Fig. 11 Arrhenius plot of heating rate, temperature of constant conversion data ($\alpha = 0.05$), alkylated hydrogenated cardanol

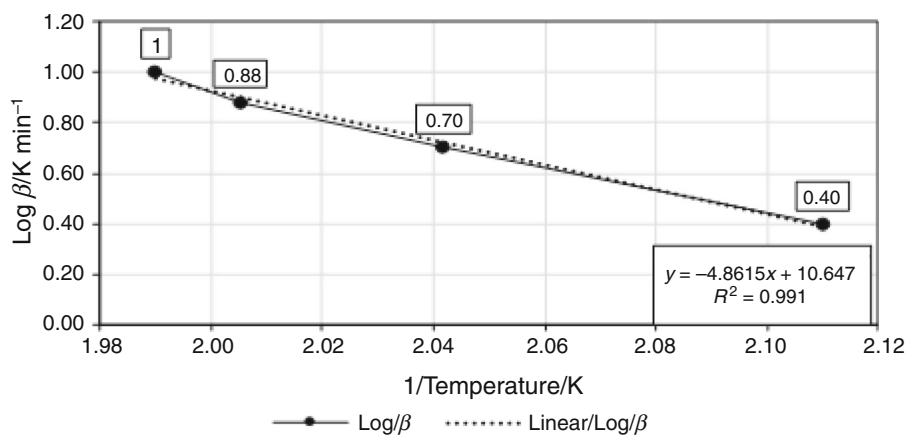


Fig. 12 Arrhenius plot of heating rate, temperature of constant conversion data ($\alpha = 0.05$), butylated hydroxytoluene

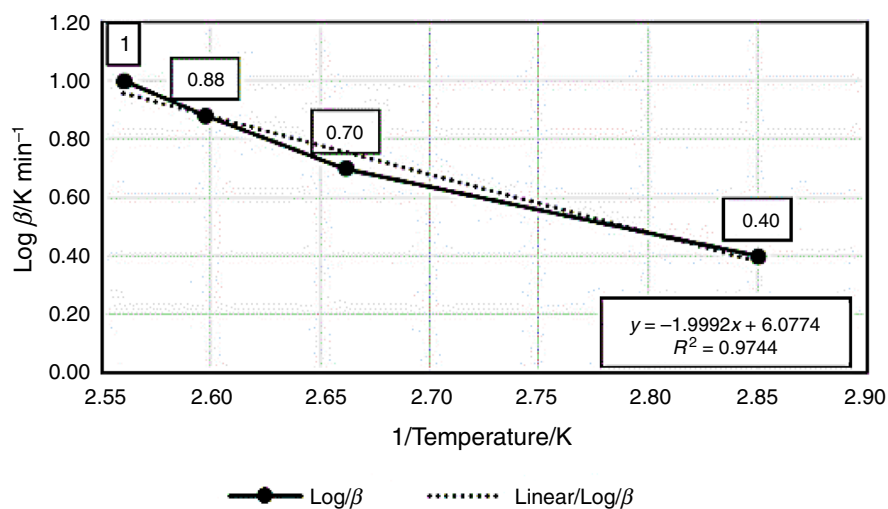


Table 3 Calculation for activation energy (E)—hydrogenated cardanol

First iteration	Second iteration	Third iteration
Slope = -2.469×10^3	Slope = -2.469×10^3	Slope = -2.469×10^3
$b = 0.457/K$	$b = 0.505/K$	$b = 0.5122/K$
$E = 44.92 \times 10^3 \text{ J mol}^{-1}$	$E = 40.65 \times 10^3 \text{ J mol}^{-1}$	$E = 40.08 \times 10^3 \text{ J mol}^{-1}$
$T_c = 453 \text{ K}$	$T_c = 453 \text{ K}$	
$E'/RT_c \approx 12$	$E/RT_c = 10.79$	

Table 4 Parameters for the calculus of pre-exponential factor (A)—hydrogenated cardanol

Parameters	Results
$\beta = 5.0 \text{ }^\circ\text{C min}^{-1}$	$A = 351.9775$
$E = 40.08 \times 10^3 \text{ J mol}^{-1}$	
$\alpha = 0.05$	$\ln A = 5.8636$
$a = 6.8206$	

Based on the results presented previously, it is suggested that the AHC is more stable than HC and BHT. Following the thermal study, the test method was used for estimating lifetimes of samples too; for this, the standard procedure described in ASTM E1877-11 was used [16]. Figures 13–15 show the thermal endurance curves of the studied samples.

The RTI is considered to be the maximum temperature below which the material resists changes in its properties over a defined period of time, and so, it is an important parameter. In this step of the work, a time to failure of 60,000 h was used for the calculus of RTI or failure

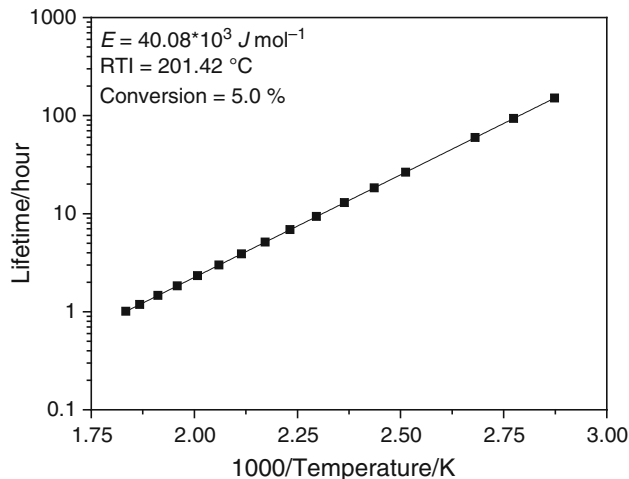


Fig. 13 Thermal endurance curve of hydrogenated cardanol

temperature T_f , obtained from the thermal endurance curve. According to the results, the HC and the AHC presented the “failure temperatures” to higher than the BHT (RTI = 166.42 °C); these results are in accordance with

Table 5 Kinetics parameters of the AHC and BHT

First iteration	Second iteration	Third iteration	Parameters	Results
<i>Alkylated hydrogenated cardanol (AHC)</i>				
Slope = -4.773×10^3	Slope = -4.773×10^3	Slope = -4.773×10^3	$\beta = 5.0 \text{ }^\circ\text{C min}^{-1}$ $E = 83.02 \times 10^3 \text{ J mol}^{-1}$ $\alpha = 0.05$ $a = 11.5584$	$A = 9.291 \times 10^6$ $\ln A = 16.0445$
$b = 0.457/K$	$b = 0.4744/K$	$b = 0.4760/K$		
$E = 86.83 \times 10^3 \text{ J mol}^{-1}$	$E = 83.43 \times 10^3 \text{ J mol}^{-1}$	$E = 83.02 \times 10^3 \text{ J mol}^{-1}$		
$T_c = 490 \text{ K}$	$T_c = 490 \text{ K}$			
$E/RT_c = 21.31$	$E/RT_c = 20.53$			
<i>Butylated hydroxytoluene (BHT)</i>				
Slope = -2.062×10^3	Slope = -2.062×10^3	Slope = -2.062×10^3	$\beta = 5.0 \text{ }^\circ\text{C min}^{-1}$ $E = 33.48 \times 10^3 \text{ J mol}^{-1}$ $\alpha = 0.05$ $a = 6.8564$	$A = 351.9775$ $\ln A = 6.1260$
$b = 0.457/K$	$b = 0.505/K$	$b = 0.5121/K$		
$E = 37.51 \times 10^3 \text{ J mol}^{-1}$	$E = 33.95 \times 10^3 \text{ J mol}^{-1}$	$E = 33.48 \times 10^3 \text{ J mol}^{-1}$		
$T_c = 376 \text{ K}$	$T_c = 376 \text{ K}$			
$E/RT_c \approx 12$	$E/RT_c = 10.86$			

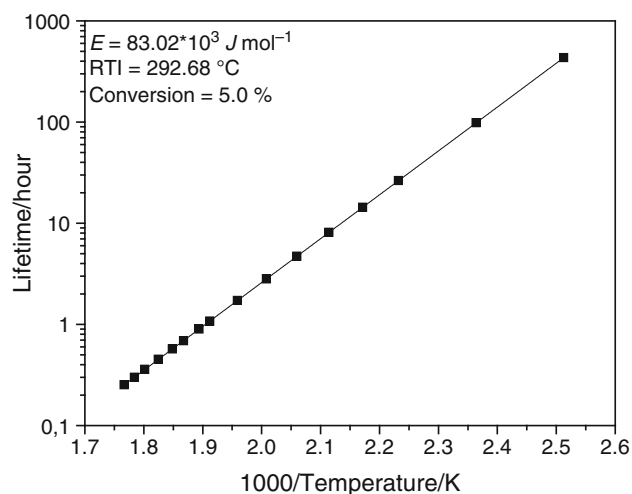


Fig. 14 Thermal endurance curve of alkylated hydrogenated cardanol

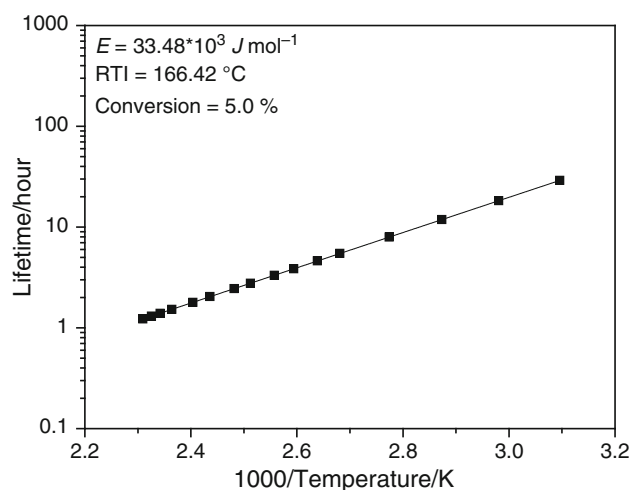


Fig. 15 Thermal endurance curve of butylated hydroxytoluene

the TG curves (see Figs. 4–6) that showed that the AHC possesses the major thermal stability.

Conclusions

The HC and its derivative compound—AHC—showed good thermal stabilities when compared to the BHT. The thermogravimetric curves for the AHC indicated a stable behavior until 178.5 °C, when initiating the thermal degradation of the medium volatile matter. In this work, the evaluation of the application of thermal analysis in the thermal endurance estimation was executed, and for the organic compounds studied (HC, AHC, and BHT), the results were satisfactory. These informations are very important because the phenols studied showed in their

structures antioxidant potentialities, and a high thermal stability is an indicator of good performance. It must be emphasized here that the thermal analysis represents a significant time-saving technique when compared with other techniques of thermal endurance and life test of organic materials. So, its use should become a more frequent and normal occurrence.

Acknowledgements The authors acknowledge CNPq (Process Number 476568/2010-2) for the financial support and the LIMAv of Federal University of Piauí for thermal analyses.

References

- Rios Façanha MA, Mazzetto SE, Carioca JOB, de Barros GG. Evaluation of antioxidant properties of a phosphorated cardanol compound on mineral oils (NH10 and NH20). *Fuel*. 2007;86(15):2416–21. doi:10.1016/j.fuel.2007.01.034.
- Bhatnagar VM, Vergnaud JM. DTA and DSC studies on polymers containing fire retardants. *J Therm Anal*. 1983;27(1):159–200. doi:10.1007/BF01907332.
- Ramani R, Alam S. Influence of an organophosphonite antioxidant on the thermal behavior of PEEK/PEI blend. *Thermochim Acta*. 2012;550:33–41. doi:10.1016/j.tca.2012.09.023.
- Rabelo Neto RC, Lima DO, Pinheiro TDS, Almeida RF, Castro Dantas TN, Dantas MSG, et al. Thermo-Oxidative Stability of Mineral Naphthenic Insulating Oils: combined Effect of Antioxidants and Metal Passivator. *Ind Eng Chem Res*. 2004;43(23):7428–34. doi:10.1021/ie049645o.
- Tychopoulos V, Tyman JHP. Long chain phenols—the thermal and oxidative deterioration of phenolic lipids from the cashew (*Anacardium occidentale*) nut shell. *J Sci Food Agric*. 1990;52(1):71–83. doi:10.1002/jsfa.2740520109.
- Rodrigues FMG, Souza AG, Santos IMG, Bicudo TC, Silva MCD, Sinfrônio FSM, et al. Antioxidative properties of hydrogenated cardanol for cotton biodiesel by PDSC and UV/VIS. *J Therm Anal Calorim*. 2009;97(2):605–9. doi:10.1007/s10973-008-9600-3.
- Maia FJN, Ribeiro VGP, Lomonaco D, Luna FMT, Mazzetto SE. Synthesis of a new thiophosphorylated compound derived from cashew nut shell liquid and study of its antioxidant activity. *Ind Crops Prod*. 2012;36(1):271–5. doi:10.1016/j.indcrop.2011.10.019.
- Mazzetto SE, Lomonaco D, Mele G. Cashew nut oil: opportunities and challenges in the context of sustainable industrial development. *Quim Nova*. 2009;32:732–41.
- Ionashiro M. “Giolito”: fundamentals of thermogravimetry, differential thermal analysis/differential scanning calorimetry. São Paulo: Giz Editorial; 2004. p. 80.
- Leiva CRM, Crnkovic PM, dos Santos AM. The employment of thermogravimetry to determine activation energy in the combustion process of fuel oils. *Quim Nova*. 2006;29:940–6.
- Standard test method for decomposition kinetics by thermogravimetry using the Ozawa/Flynn/Wall Method. West Conshohocken: ASTM International; 2013; p. 6.
- Muraleedharan K, Kripa S. DSC kinetics of the thermal decomposition of copper(II) oxalate by isoconversional and maximum rate (peak) methods. *J Therm Anal Calorim*. 2014;115(2):1969–78.
- Chen Z, Xia Y, Liao S, Huang Y, Li Y, He Y, et al. Thermal degradation kinetics study of curcumin with nonlinear methods. *Food Chem*. 2014;155:81–6.

14. Shadangi KP, Mohanty K. Kinetic study and thermal analysis of the pyrolysis of non-edible oilseed powders by thermogravimetric and differential scanning calorimetric analysis. *Renew Energy*. 2014;63:337–44. doi:[10.1016/j.renene.2013.09.039](https://doi.org/10.1016/j.renene.2013.09.039).
15. Ravi P, Vargeese AA, Tewari SP. Isoconversional kinetic analysis of decomposition of nitropyrazoles. *Thermochim Acta*. 2012;550:83–9. doi:[10.1016/j.tca.2012.10.003](https://doi.org/10.1016/j.tca.2012.10.003).
16. Standard practice for calculating thermal endurance of materials from thermogravimetric decomposition data. West Conshohocken: ASTM International; 2013. p. 6.
17. Standard test method for compositional analysis by thermogravimetry. West Conshohocken: ASTM International; 2014. p. 5.
18. Rios MAD, Sales FAM, Mazzetto SE. Study of antioxidant properties of 5-n-pentadecyl-2-tert-amylphenol. *Energy Fuels*. 2009;23:2517–22. doi:[10.1021/ef800994j](https://doi.org/10.1021/ef800994j).
19. Rios MADS, Santiago SN, Lopes AAS, Mazzetto SE. Antioxidative activity of 5-n-pentadecyl-2-tert-butylphenol stabilizers in mineral lubricant oil. *Energy Fuels*. 2010;24(5):3285–91.
20. Toop DJ. Theory of life testing and use of thermogravimetric analysis to predict thermal life of wire enamels. *IEEE Trans Electr Insul*. 1971;6(1):2–14. doi:[10.1109/tei.1971.299128](https://doi.org/10.1109/tei.1971.299128).
21. Krizanovsky L, Mentlik V. Use of thermal-analysis to predict thermal life of organic electrical insulating materials. *J Therm Anal Calorim*. 1978;13(3):571–80.
22. Tomassetti M, Favero G, Campanella L. Kinetic thermal analytical study of saturated mono-, di- and tri-glycerides. *J Therm Anal Calorim*. 2013;112(1):519–27. doi:[10.1007/s10973-012-2821-5](https://doi.org/10.1007/s10973-012-2821-5).
23. Dirion J-L, Reverte C, Cabassud M. Kinetic parameter estimation from TGA: optimal design of TGA experiments. *Chem Eng Res Des*. 2008;86(6):618–25. doi:[10.1016/j.cherd.2008.02.001](https://doi.org/10.1016/j.cherd.2008.02.001).
24. Sousa Rios MA, Mazzetto SE. Thermal behavior of phosphorus derivatives of hydrogenated cardanol. *Fuel Process Technol*. 2012;96:1–8. doi:[10.1016/j.fuproc.2011.12.004](https://doi.org/10.1016/j.fuproc.2011.12.004).
25. Sousa Rios M, Mazzetto S. Effect of organophosphate antioxidant on the thermo-oxidative degradation of a mineral oil. *J Therm Anal Calorim*. 2013;111(1):553–9. doi:[10.1007/s10973-011-2160-y](https://doi.org/10.1007/s10973-011-2160-y).